15th International Conference on Recent Trends in Engineering, Applied Science and Management
Gurukul Institute of Engineering & Technology, Rajasthan, India. ICRTEASM-18
1st April 2018 www.conferenceworld.in ISBN: 978-93-87793-18-7

# DESIGN ANALYSIS OF A 3-DOF PARALLEL ROBOT FOR ACCURATE POSITION OF AN ASTRONOMICAL SPATIAL TELESCOPE

***Bharat Kumar Sahu[1], Deepak Jatil[2], Akshay Sharma[3], Abhinav Swami[4]**

*Department of Mechanical Engineering*

*Gurukul Institute of Engineering & Technology, Kota*

## ABSTRACT

*The extents of motion available in different directions are quite different and that the overall telescope position range of motion is rather small. Since the robot should be able to cater for both the left and right legs, the different motion limits in the roll and internal-external rotation directions will be inverted in the robot coordinate frame when a foot from the different side of the body is placed on the robot. The limits of the required robot rotational workspace on the frontal and transverse planes are therefore symmetric. The robot used in this research was therefore designed by assuming that the maximum internal/external rotation moments are similar in magnitude to the roll moments.*

## I.INTRODUCTION

Parallel robots have a kinematic structure whereby the end effector is connected to a fixed base through multiple actuated links. Due to this arrangement, parallel robots have several advantages over their serial counterparts. One of these advantages is higher positioning accuracy since errors in the actuated joints no longer accumulate as in the case of serial robots. Furthermore, since the end effector is supported by multiple actuators, the load capacity of the mechanism can also be increased. As actuators of a parallel robot is located at its base rather than on its moving links, the total load moved by the manipulator is also reduced.

## II.DETERMINATION OF A SUITABLE ROBOT KINEMATIC STRUCTURE

The mobility or number of degrees of freedom available in a spatial mechanism is given by the Grubler's mobility formula shown in equation (1) [1], where $M$ is the mobility of the mechanism, $n$ is the number of rigid links present in the mechanism (including the fixed base), $g$ is the total number of active and passive joints and $f_i$ is the degree of freedom for the $i^{th}$ joint.

$$M = 6(n - g - 1) + \sum_{i=1}^{i=g} f_i \qquad (1)$$

In the proposed setup, the foot of the user is attached to the end effector and the shank is attached to the base of the mechanism. In the absence of any actuating links, the only kinematic constraint between the base and the

end effector will be the human telescope position joint. In this scenario, $n_0$ = 2 and $g_0$ = 1. Consequently, the mobility of this mechanism, $M_0$, is identical to that of the natural telescope position joint. Clearly, actuated links must be included in the mechanism to allow control of the device, however, it should be noted that the mobility after the addition of actuated links must be identical to $M_0$ if the natural motion of the foot is to be preserved.

## III.WORKSPACE, SINGULARITY AND FORCE ANALYSES

Due to the incorporation of the human telescope position as part of the parallel mechanism, its kinematic description must be established prior to any analyses on the workspace, singularities and moment capabilities of the telescope position robot. Although foot motion is often depicted through rotations about two oblique revolute joints in series [2-4], its actual movement pattern appears to be more complicated with coupled translations and rotations. Studies had found that the orientations of the revolute joints in the biaxial model can vary significantly between individuals.

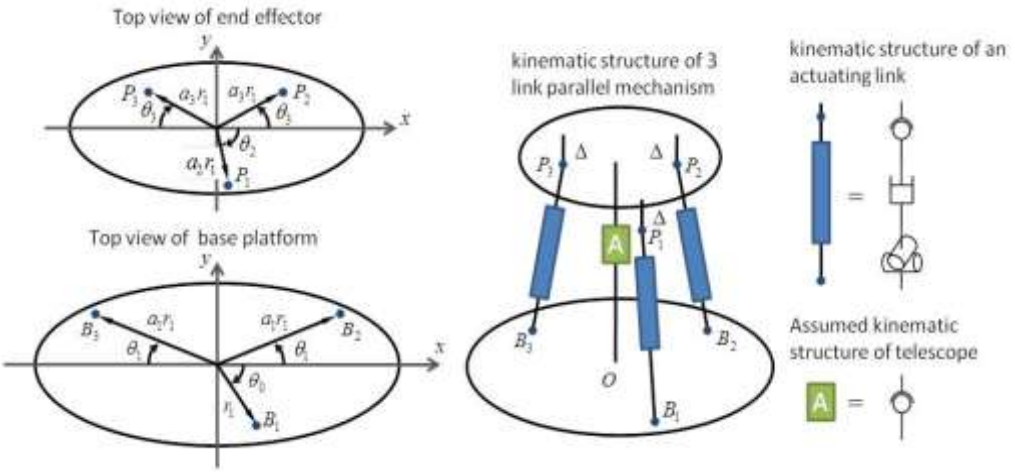


Figure 1**:** Kinematic structure of the three link parallel mechanism with central strut

In Figure 1, the attachment points of the actuated links on the base are denoted by $B_i$ while their attachments on the end effector are represented by $P_i$. Based on the U<u>P</u>S link structure, point $B_i$ is coincident with the centre of the universal joint while point $P_i$ is coincident with the centre of the spherical joint or equivalent on the $i^{th}$ actuated link. Point $O$ had also been defined on the base platform where it acts as the origin of the robot global coordinate frame. The points $B_i$ and $O$ are constrained to lie on the same plane and their relative positions are parameterised in polar coordinates. The projections of points $P_i$ on the end effector can similarly be represented in polar coordinates. In addition to that, the distance between $P_i$ and the end effector plane is also set to be constant for all $i$, and is denoted by Δ. Finally, the point $A$ is defined as the centre of the spherical joint used to represent the human telescope position.

## IV.INVERSE KINEMATICS

The inverse kinematics of a parallel mechanism is the mapping that relates a particular end effector orientation to its corresponding joint displacements in terms of lengths of the actuated links. Such a relationship can be easily established using the kinematic parameters described above. By using the subscript 0 to represent quantities relating to the zero orientation, a pose where the end effector orientation is identical with that of the robot global frame, the link vector of the $i^{th}$ actuated link can be written as equation (2), while its length is given by equation (3).

$$L_i = \overrightarrow{OA} + R\left(\overrightarrow{AP_{i,0}}\right) - \overrightarrow{OB} \tag{2}$$

$$l_i = \sqrt{L_i{}^T L_i} \tag{3}$$

### Computation of reachable workspace

Results obtained from the inverse kinematics are highly relevant for the determination of the workspace available in the parallel mechanism. Assuming that the passive joints have been selected so that the limiting factor on the robot workspace is solely that of the length of the actuated prismatic joint, an end effector orientation can only pass as a point in the robot workspace if all the actuated link lengths fall within an allowable range. This range is typically controlled by the retracted and extended lengths of the linear actuator used in the link. For the purpose of initial analysis, it is assumed that the permissible ranges for the actuator lengths are centred about their respective values at the zero orientation. More precisely, the inequality denoting the constraint on actuated link lengths can be given as equation (4), where $\Delta l_{max}$ is the maximum stroke length of the linear actuator and $l_{i,0}$ is the length of the $i^{th}$ actuated link at the zero orientation.

$$l_{i,0} - 0.5\Delta l_{max} \leq l_i \leq l_{i,0} + 0.5\Delta l_{max} \tag{4}$$

### Computation of singularity measure

The manipulator Jacobian is a matrix which describes the relationship between joint space and task space velocities of a robot. For parallel mechanisms where a unique set of joint space coordinates can be assigned to a given task space configuration, the manipulator Jacobian $J$ is the gradient matrix which relates the task space velocity $\dot{\Theta}$ to the joint space velocity $\dot{l}$ as shown in equation (5). It is also worth noting that the transpose of the manipulator Jacobian is used to relate the joint space forces $F$ to task space forces $\tau$, as shown in equation (6). Analysis of the manipulator Jacobian can therefore provide information on the kinematics and kinetics of a robot at a particular configuration. The manipulator Jacobian for the proposed parallel kinematic structure can be obtained from differentiation of the inverse kinematics relationship shown in equation (7).

$$\dot{l} = J\dot{\Theta} \tag{5}$$

$$\tau = J^T F \tag{6}$$

$$J_i = \frac{1}{l_i} L_i{}^T \left[ \frac{\partial R}{\partial \theta_x} P_{i,0} \quad \frac{\partial R}{\partial \theta_y} P_{i,0} \quad \frac{\partial R}{\partial \theta_z} P_{i,0} \right] \tag{7}$$

An important role of the manipulator Jacobian is in the identification of singular configurations of the robot. Singular configurations are poses of the robot whereby the manipulator Jacobian is rank deficient. This means that singular configurations are generally related to an infinite condition number or zero matrix determinant if the manipulator Jacobian is a square matrix. Rank deficiency in the manipulator Jacobian will lead to the loss of controllability of the robot, where the realisation of task space forces along certain directions will not be possible regardless of the joint space forces being applied. As a result, a good design should aim to improve the manipulability of the robot by reducing the condition numbers of manipulator Jacobian across all points in the task space.

## V.FORCE ANALYSIS

In the force analysis, the vectors along which moments are applied were different for different foot configurations considered. The main motivation for this arrangement is to reduce the number of computations required in the analysis by only applying forces in directions where they are expected at a particular configuration. Since the foot will have a tendency to move towards the neutral position, passive motion of the foot will be initiated by the robot applying a force in the direction where it is moving. The opposite however is true for active exercises where the robot is providing a resistive force. In either case, the direction of moment application should be similar to the direction of the position vector taken from the zero orientation to the foot configuration being considered e.g. force analysis for a pitch up flexed foot orientation should involve application of moments in the pitch up-pitch down direction. The exception for this is of course the neutral position, where a much larger range of moments in terms of direction can be applied to move or resist the motion of the foot.

## VI.ANALYSIS RESULTS AND DISCUSSION

Apart from the workspace, singularity and force requirements, the resultant design must also meet certain spatial constraints to ensure that it can be used in practice. Since the robot developed in this research is used for telescope position, the kinematic parameters of the robot must be selected in such a way that it can accommodate the placement of the foot on the end effector. With this in mind, several sets of kinematic parameters for the proposed three link parallel mechanism had been selected and analysed.

**Table** 1**:** Kinematic parameters for the three link parallel mechanism

| Parameter | $r_1$ | $a_1$ | $a_2$ | $a_3$ | $\theta_0$ | $\theta_1$ | $\theta_2$ | $\theta_3$ | $\Delta$ | $\overrightarrow{OA}$ |
|---|---|---|---|---|---|---|---|---|---|---|
| Value | 0.2 m | 0.9 | 0.4 | 0.45 | -90° | 45° | -90° | 30° | 0.05 m | [0 0 0.36] m |

For illustrative purposes, the results for one of these mechanisms which kinematic parameters are given in Table are shown in Figure to Figure . Figure shows a slice of the robot workspace when the rotation about the Z Euler axis is zero. An inspection of this plot shows that this robot configuration can produce about 32° and 36° of maximum pitch up and pitch down respectively. Additionally, the maximum roll motion is around 36°. A three dimensional view of workspace volume is also shown in Figure , and it can be seen that the largest range of motion of the robot is by far in the yaw direction, with maximum rotations of over 90°. The workspace regions with low manipulability are also indicated by the red point clouds in Figure where they appear to form a region/surface which separates the workspace in two.

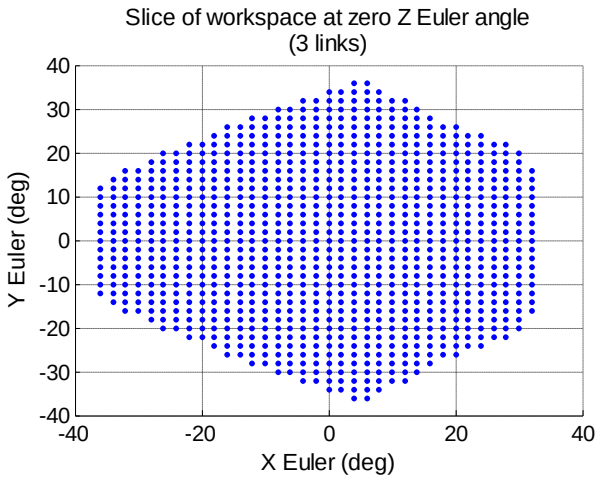


Figure 2**:** A slice of the robot workspace at zero Z Euler angle for the three link parallel mechanism.

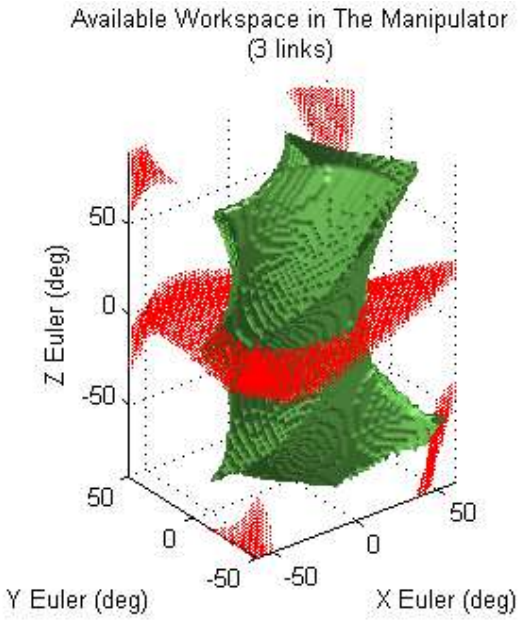

Figure 3**:** Superposition of the workspace volume on regions of the task space with low manipulability (configurations where condition number >50) for the three link parallel mechanism.

A better visualisation of the task space configurations with low manipulability is given in the volumetric plot shown in Figure . In this plot, the condition numbers of the manipulator Jacobians at different orientations are represented in a colour spectrum and plotted on the three dimensional axes. In addition to the colour coding, the transparency of the points are also affected by the condition numbers, where configurations with lower condition number is assigned a higher transparency. Using this arrangement, regions with low manipulability becomes more easily identifiable. It should also be noted that to allow better visualisation, the colour coding was done in the base 10 logarithmic scale and the condition numbers were saturated at 1000.

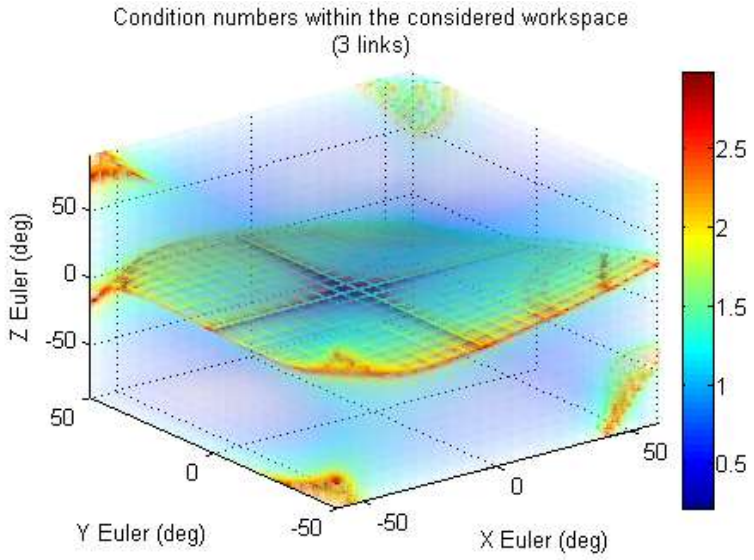


Figure 4**:** Plot indicating the distribution of manipulator Jacobian condition numbers throughout the manipulator task space for the three link parallel mechanism. The colour spectrum is assigned to the base 10 logarithms of the condition numbers.

## REFERENCES

1. J.-P. Merlet, *Parallel robots*, Second ed. Netherlands: Springer, 2006.
2. L.-W. Tsai, Robot analysis: the mechanics of serial and parallel manipulators. New York: John Wiley & Sons, 1999.
3. J. Dul and G. E. Johnson, "A kinematic model of the human ankle," *Journal of Biomedical Engineering*, vol. 7, pp. 137-143, 1985.
4. Jorge Angeles, "Fundamentals of Robotic Mechanical Systems", *Springer*, 3rd Edition, McGill University, Montreal, Quebec, Canada, 2007.
5. Pashkevich, D. Chablat and P. Wenger, "Kinematics and workspace analysis of a three-axis parallel manipulator: the Orthoglide, Robotica", *Cambridge University Press*, vol.24, no.1, 2006.

6. K. M. Lee and D. K. Shah, "Kinematic Analysis of a Three-Degrees-of-Freedom In-Parallel Actuated Manipulator", *IEEE JOURNAL OF ROBOTICS AND AUTOMATION*, Vol. 4, No. 3, pp. 354-360, 1988.
7. Serdar Kucuk and Zafer Bingul, "Robot Kinematics: Forward and Inverse Kinematics", *Industrial-Robotics-Theory-Modelling- control*, ISBN 386611-285-8, pp. 964, Germany, December 2006.
8. P.K. Mittal and I.J. Nagrath, "Robotics and control", *Tata McGraw Hill*, 13th Edition, 2009.